Acta Biochim Biophys Sin, 2021, 53(11), 1428–1439
https://doi.org/10.1093/abbs/gmab122
Advance Access Publication Date: 11 September 2021
Original Article

Original Article

Aryl hydrocarbon receptor signaling pathway plays important roles in the proliferative and metabolic properties of bone marrow mesenchymal stromal cells

Yan Jia, Youshan Zhao, Zheng Zhang, Lei Shi, Ying Fang, and Chunkang Chang*

Department of Hematology, Shanghai Jiao Tong University Affiliated Sixth People's Hospital, Shanghai 200233, China
*Correspondence address. Tel: +86-13764643870; E-mail: changchunkang@sjtu.edu.en

Received 2 March 2021; Editorial Decision 27 May 2021

Abstract

Bone marrow mesenchymal stromal cells (BMMSCs) are widely sourced and easily amplified *in vitro*; thus, they have a great potential in the treatment of hemopathies. Recent findings suggested that BMMSCs express the aryl hydrocarbon receptor (AHR). However, few studies have reported on the regulation of proliferative behaviors and metabolism by AHR in BMMSCs. In the present study, we found that activating AHR reduced the proliferation of BMMSCs and enhanced their mitochondrial function, whereas inhibiting AHR exerted the opposite effects. This study may provide the basis for further unveiling the molecular mechanisms and therapeutic potential of AHR in BMMSCs.

Key words: AHR, BMMSC, mitochondrial metabolism, proliferation

Introduction

As important components of the bone marrow microenvironment, bone marrow mesenchymal stromal cells (BMMSCs) modulate hematopoiesis and immunity via direct contact or the secretion of adhesion factors and hematopoietic chemokines [1]. Under specific pathological circumstances, BMMSCs may also facilitate damage to the hematopoietic and immune systems [2–5]. In hemopathy patients, the quality and quantity of BMMSCs are abnormal. Previous studies demonstrated that BMMSCs from myelodysplastic syndrome (MDS) patients and multiple myeloma patients display significantly increased senescence and are unable to provide sufficient hematopoietic support [6,7]. Crippa *et al.* [8] found that bone marrow stromal cells from β-thalassemia patients have impaired hematopoietic supportive capacity. The dysfunction of BMMSCs impairs bone marrow microenvironment, which promotes leukemia development and is involved in chemotherapeutic resistance [9]. In other words, BMMSCs dysfunction plays important roles in the occurrence and development of hematological diseases.

Recent studies showed that BMMSCs have therapeutic potential in hematological diseases. For example, transfusion of healthy BMMSCs into bone marrow can restore the local bone marrow microenvironment, as demonstrated by the functional recovery of host BMMSCs, restored myelopoietic balance, and improved thrombopoiesis [10]. In leukemia-bearing mice, BMMSCs therapeutically reduced tumor burden and prolonged the survival [10]. Adoptive healthy BMMSC infusion can be exploited to heal the 'sick' niche in MDS and aplastic anemia patients, which can enhance the effect of allogeneic hematopoietic stem cell transplantation (HSCT) [11].

HSCT is an effective treatment for hematological diseases. However, the effectiveness and use of HSCT are limited by lethal complications, including chronic and acute graft-versus-host disease (GVHD), in which immune cells from the donor attack healthy recipient tissues [12]. GVHD is a vast challenge in the application of HSCT, and the overall survival is poor [13]. BMMSCs were also demonstrated to have considerable promise for both the prevention and treatment of GVHD because of their potential immunomodulatory activity [14,15]. In addition, due to the important roles of BMMSCs in HSC niches, where they support hematopoiesis, BMMSCs promote HSC engraftment following transplantation [16,17]. As our knowledge of BMMSCs grows, they are considered increasingly to be useful tools for preventing and treating GVHD in the

HSCT setting and have been approved for use as immunomodulators in clinical trials [18].

The aryl hydrocarbon receptor (AHR), which belongs to the basic helix-loop-helix/Per-Arnt-Sim (bHLH/PAS) family, is an important cytosolic, ligand-dependent transcription factor [19]. Recent findings revealed that BMMSCs express AHR, and the activation of the AHR in these cells plays roles in inflammation and immunomodulation via paracrine effects [20]. Previous studies have shown that AHR attenuates oxidative-stress-induced injury in cells by maintaining the structure and function of mitochondria [21–23]. Zhou *et al.* [24] showed that knocking down the AHR gene in mast cells reduced oxidative phosphorylation. Mitochondrial transcription factor A (TFAM), initially discovered as a transcription factor for mitochondrial DNA (mtDNA), is critical in mitochondrial function [25,26]. The maintenance of mtDNA stability is primarily mediated by TFAM, and it is required for mtDNA replication and transcription [27]. Under pathological conditions, disruption of TFAM could lead to mitochondrial mtDNA depletion and deficient mitochondrial bioenergetics [28]. Studies have demonstrated that TFAM is involved in mitochondrial energy metabolism, and the loss of TFAM decreases the oxidative phosphorylation [29–31]. Activation of AHR in human melanocytes through TFAM enhances the mitochondrial function against oxidative damage [32]. Moreover, in our previous studies, we found that activating AHR enhanced the mitochondrial function accompanied by increased TFAM expression [33]. However, few studies have focused on the regulation of proliferative behaviors and metabolism by AHR in BMMSCs.

There are few BMMSCs in the bone marrow; therefore, their *ex vivo* expansion is required before they can be used in clinical trials [34]. It is recognized that the switch of energy supply from glycolysis to aerobic metabolism is essential for the differentiation of MSCs [35]. Accumulating evidence has demonstrated that the therapeutic potential of BMMSCs is associated with mitochondrial function [36,37].

In the present study, we found that activating the AHR in BMMSCs inhibited their proliferation and reshaped their metabolism. Our results may provide the basis for further unveiling the molecular mechanisms and therapeutic potential of the AHR in BMMSCs.

Materials and Methods

Study participants

Six healthy volunteers participated in the study (three females and three males; age range, 25–45 years). All the participants provided informed consent prior to their inclusion in the study. The present protocol received the approval from the Ethics Committee of the Sixth People's Hospital affiliated to Shanghai Jiao Tong University (SH6THHOSP-YS-2020-118).

Isolation and culture of human BMMSCs

Bone marrow mononuclear cells (BMMNCs) were isolated from fresh bone marrow aspirates using Ficoll-Paque Plus (GE Healthcare, Uppsala, Sweden). BMMNCs were seeded at a density of 1×10^6 cells/ml in human mesenchymal stem cell growth medium (Cyagen Biosciences Inc., Guangzhou, China) supplemented with 10% fetal bovine serum (Gibco, Grand Island, USA), glutamine, and 100 U/ml penicillin/streptomycin (Beyotime Biotechnology, Haimen, China). Cells were maintained at 37°C in a humidified atmosphere with 5% CO_2. After 24 h of incubation, the culture medium was refreshed and the non-adherent cells were removed. In the subsequent experiments, SR1 (Selleck, Shanghai, China) was used to inhibit AHR activation. L-Kynurenine (Santa Cruz Biotech, Santa Cruz, USA) was used to activate AHR.

Identification of BMMSCs

BMMSCs were cultured up to the third generation and then examined under a light microscope. The morphology of the BMMSCs was long and fusiform. Cell surface markers, including CD29, CD73, CD90, CD105, CD166, CD31, CD34, CD45, CD11b, and human leukocyte antigen (HLA)-DR, were detected by flow cytometry on a BD flow cytometer (BD Biosciences, Franklin Lakes, USA). The operations were performed according to the manufacturer's instructions. All antibodies were purchased from BD.

Cell lines and culture conditions

HS-27A cells (provided by Dr Lei Shi, Shanghai Jiao Tong University, Shanghai, China), which were derived from bone marrow and had the same characteristics as BMMSCs, were used in this study. The HS-27A cells were seeded at a density of 2×10^5 cells/ml and cultured in Roswell Park Memorial Institute (RPMI)-1640 medium (JiRuo Company, Hangzhou, China) supplemented with 10% fetal bovine serum and 5% penicillin–streptomycin at 37°C in a humidified atmosphere with 5% CO_2. SR1 was used to inhibit AHR activation. L-Kynurenine was used to activate AHR.

Cell proliferation assay

Cells were seeded at a density of 2×10^5 cells/ml into 24-well plates, and cell viability was detected after 24, 48, and 72 h. The cells were stained with trypan blue (Solarbio, Beijing, China) by mixing the cell suspension and trypan blue solution at a ratio of 9:1 and dropped onto a hemocytometer. The average numbers of unstained cells and total cells were counted, and the percentage of unstained cells denotes the cell viability. Relative cell multiplication was determined as the ratio of the number of cells in the experimental group compared to that in the control group.

The CFDA SE Cell Proliferation kit (YESEN, Shanghai, China) was used to assess cell proliferation according to the manufacturer's protocol. CFDA and SE can enter cells through the permeability of cell membrane. After entering the living cells, they can be catalyzed by the esterase to produce carboxyfluorescein succinimidyl ester (CFSE). CFSE is an effective and popular means to monitor cell division. CFSE covalently labels long-lived intracellular molecules with the fluorescent dye, carboxyfluorescein. Thus, when a CFSE-labeled cell divides, its progeny is endowed with half the number of carboxyfluorescein-tagged molecules and thus each cell division can be assessed by measuring the corresponding decrease in cell fluorescence via the flow cytometer. ModFit software was used to analyze the data.

Apoptosis and cell cycle analysis

Cell apoptosis was detected using an Annexin V–FITC kit (BD Biosciences) following the manufacturer's protocol. The apoptotic cells were examined using the flow cytometer. Cell cycle and apoptosis analysis kits (Solarbio) were used to detect the cell cycle following the manufacturer's protocols. ModFit software was used to analyze the data.

Colony formation assay

Cells were seeded into 6-well plates (500 cells/well) and cultured in 3 ml of RPMI-1640 medium supplemented with 10% fetal bovine serum and 5% penicillin–streptomycin and gently rotated to evenly

disperse the cells. The culture process continued at 37°C in a humidified atmosphere with 5% CO_2 for 2–3 weeks. When visible clones appeared in the plate, the supernatant was discarded and the cells were carefully washed twice with phosphate buffered saline (PBS). Then, 3 ml of 4% paraformaldehyde was added to each well and incubated for 15 min to fix the cells. The fixative was removed and Giemsa (Biyuntian, Shanghai, China) was added to stain the cells for 10–30 min, followed by a slow wash with running water. The cells were slowly dried at room temperature, and the number of clones was counted under a light microscope at 10× magnification. Finally, the colony formation rate was calculated as follows: colony formation rate (%)=(number of clones/number of inoculated cells)×100%.

Measurement of mitochondrial dehydrogenase level and pH value

The cells in the logarithmic growth phase were selected and suspended in human mesenchymal stem cell growth medium at a density of 2×10^5 cells/ml. The 2-(2-methoxy-4-nitrophenyl)-3-(4-nitrophenyl)-5-(2,4-disulfonate)-2H-tetrazole monosodium salt kit (Dojindo, Tokyo, Japan) was used to detect the content of mitochondrial dehydrogenase. In the presence of 1-methoxy-5-methylphenazine and 1-methoxy phenazinium methylsulfate, WTS-8 redox with the dehydrogenase in the mitochondria produces a highly water-soluble yellow manicure product (Formazan). Briefly, cell suspension was mixed with WTS-8 at 9:1 (v/v) and incubated at 37°C in a humidified atmosphere of 5% CO_2 for 2 h. The optical density was detected at 450 nm using a microplate reader following the instructions provided with the kit.

Cells in the logarithmic growth phase were selected and suspended in RPMI-1640 medium containing phenol red at a density of 2×10^5 cells/ml. After 72 h of incubation, color changes in media were observed and images were captured. The cell suspension was centrifuged for 5 min at 1000 rpm in a sterile centrifuge tube and the supernatant was collected. The pH value of the media was measured using a pH pen (Bangte, Beijing, China) according to the manufacturer's instructions.

Detection of L-lactate

BMMSCs were cultured for 72 h and the culture medium was collected. L-Lactate in the culture medium was detected using an L-lactate assay kit (BioAssay Systems, Hayward, USA) according to the manufacturer's instructions.

Detection of mitochondrial membrane potential

The mitochondrial membrane potential (MMP) was detected using the MMP kit (JC-1; Beyotime Biotechnology) according to the manufacturer's protocol. When the MMP is low, JC-1 cannot aggregate in the matrix of the mitochondria and remains a monomer, which produces green fluorescence. When the MMP is high, JC-1 accumulates in the mitochondrial matrix and forms a polymer (J-aggregate), which emits red fluorescence. In this way, JC-1 can be conveniently used to detect changes in the MMP via a change in fluorescent color. Briefly, the cells were incubated with JC-1 at 37°C for 20 min, and then washed twice with JC-1 buffer and observed under a fluorescence microscope (Zeiss, Oberkochen, Germany) at 40× magnification.

Table 1. Sequences of siRNAs used in this study

Name	Sequence (5′→3′)
Negative control-siRNA	F: UUCUCCGAACGUGUCACGUTT
	R: ACGUGACACGUUCGGAGAATT
AHR-siRNA1	F: GCUCUGAAUGGCUUUGUAUTT
	R: AUACAAAGCCAUUCAGAGCTT
AHR-siRNA2	F: CCACAUCCACUCUAAGCAATT
	R: UUGCUUAGAGUGGAUGUGGTT
AHR-siRNA3	F: CCUGUAAUCAGCCUGUAUUTT
	R: AAUACAGGCUGAUUACAGGTT

Cell transfection

BMMSCs and HS-27a cells were cultured in 24- or 6-well plates overnight and transfected with 50 nM AHR-specific small interfering RNA (siRNA) or control siRNA (Hanheng, Shanghai, China) using Lipofectamine 3000 reagent (Invitrogen, Carlsbad, USA) according to the manufacturer's instructions. AHR-targeted siRNA was diluted in reduced serum medium Opti-MEM® I medium (Gibco), gently mixed with an equal volume of Lipofectamine 3000 reagent, and incubated for 20 min at room temperature. The siRNA/Lipofectamine solution was directly added to the cells that were then incubated for 48 h. The relative expression levels of AHR were detected by quantitative reverse transcriptase-polymerase chain reaction (RT-PCR) and western blot analysis. The sequences of siRNAs are listed in Table 1.

Quantitative RT-PCR

Total RNA was extracted using an RNeasy Mini kit (Qiagen, Hilden, Germany) according to the manufacturer's instructions. A PrimeScript RT reagent kit (TaKaRa, Dalian, China) was used to synthesize complementary DNA. Quantitative polymerase chain reaction (qPCR) was conducted using Real-time PCR Master Mix (TaKaRa) on an ABI7500 real-time PCR system (Applied Biosystems, Foster City, USA). *β-Actin* was used as an endogenous control. The gene expression results were expressed relative to the expression of *β-actin*. The relative gene expression levels were calculated using the $2^{-\Delta\Delta Ct}$ method. All primer sequences used in the experiments are listed in Table 2.

Western blot analysis

For western blot analysis, cells were washed with ice-cold PBS and lysed in radioimmunoprecipitation assay buffer (Gibco) for 20 min on ice. The supernatant was obtained by centrifuging the lysate at 12,000 *g* and 4°C. Proteins were separated by sodium dodecyl sulfate-polyacrylamide gel electrophoresis and transferred to polyvinylidene difluoride membranes (Millipore, Billerica, USA). The membranes were blocked with 5% skimmed milk for 1–2 h and incubated overnight with the primary antibodies, including anti-AHR, anti-CYP1A1, anti-CYP1B1, and anti-TFAM antibodies (Abcam, Cambridge, USA). The membranes were then incubated with the corresponding horseradish-peroxidase-conjugated goat anti-rabbit immunoglobulin G secondary antibodies (Abcam) for 2 h. Protein bands were visualized using an enhanced chemiluminescence detection kit (Amersham Biosciences, Cambridge, UK). β-Actin was used as a loading control.

Table 2. Sequences of primers used in this study

Target gene	Sequence (5′→3′)
CDK1	F: CTTCACTTGTTAAGAGTTATTTATACC
	R: AATCAGCCAGTTTAATTGTTCC
CDK2	F: CTATGCCTGATTACAAGCCAAG
	R: GCTCCGTCCATCTTCATCC
CDK3	F: GCTCTTTCGTATCTTTCGTATGC
	R: CAATCTCTTCCAGTCCCTTCC
CDK4	F: TGGTGTCGGTGCCTATGG
	R: GAACTGTGCTGATGGGAAGG
CDK6	F: CTATGGGAAGGTGTTCAAGG
	R: GCGGATGGTGGAGAGC
CDK7	F: GGATGTATGGTGTAGGTGTGG
	R: TGTTCCTCAGTTGGTGTGC
CYP1A1	F: GTCTTGGACCTCTTTGGAGCT
	R: GTGACCTGCCAATCACTGTG
CYP1B1	F: GTACCGGCCACTATCACTGACA
	R: CACATCAGGATACCTGGTGAAGAG
TFAM	F: ACAGGATGATGACTATGGAA
	R: CAACTCTGAATACAATGTGAATT
β-Actin	F: CCTTCCTGGGCATGGAGTCCTG
	R: GGAGCAATGATCTTGATCTTC

Statistical analysis

Each experiment was repeated independently at least three times. Data are expressed as the mean ± standard deviation (SD). Statistical analysis was performed with SPSS 13.0 software (SPSS, Inc., IL, USA). Data comparisons were performed using Student's *t*-test. $P<0.05$ was considered statistically significant.

Results

Identification of BMMSCs

BMMSCs were cultured to the third generation and the surface markers were detected by flow cytometry. Isotype controls were used in the experiments (Fig. 1A). The BMMSCs had high expression levels of CD29, CD73, CD90, CD105, and CD166, but almost no expression of CD31, CD34, CD45, CD11b, or HLA-DR (Fig. 1B,C). These results indicated that BMMSCs were successfully cultured according to the criterion of the International Society of Cell Therapy (ISCT) for BMMSCs.

AHR in BMMSCs were inhibited or activated by SR1 or L-Kynurenine, respectively

The recognized AHR inhibitor SR1 and endogenous AHR activator L-Kynurenine were administered to HS-27a cell line and human BMMSCs to inhibit or activate AHR, respectively, for 24, 48, and 72 h. The addition of SR1 eventually led to an increase in the proliferation of HS-27a cells and BMMSCs in time- and concentration-dependent manners, but as the concentration of SR1 reached 1 μM, the proliferation began to decrease (Fig. 2A). After activating AHR with L-Kynurenine in BMMSCs and HS-27a cells, the proliferation was decreased in time- and concentration-dependent manners (Fig. 2B). Considering the toxicity of the drugs, 1 μM SR1 and

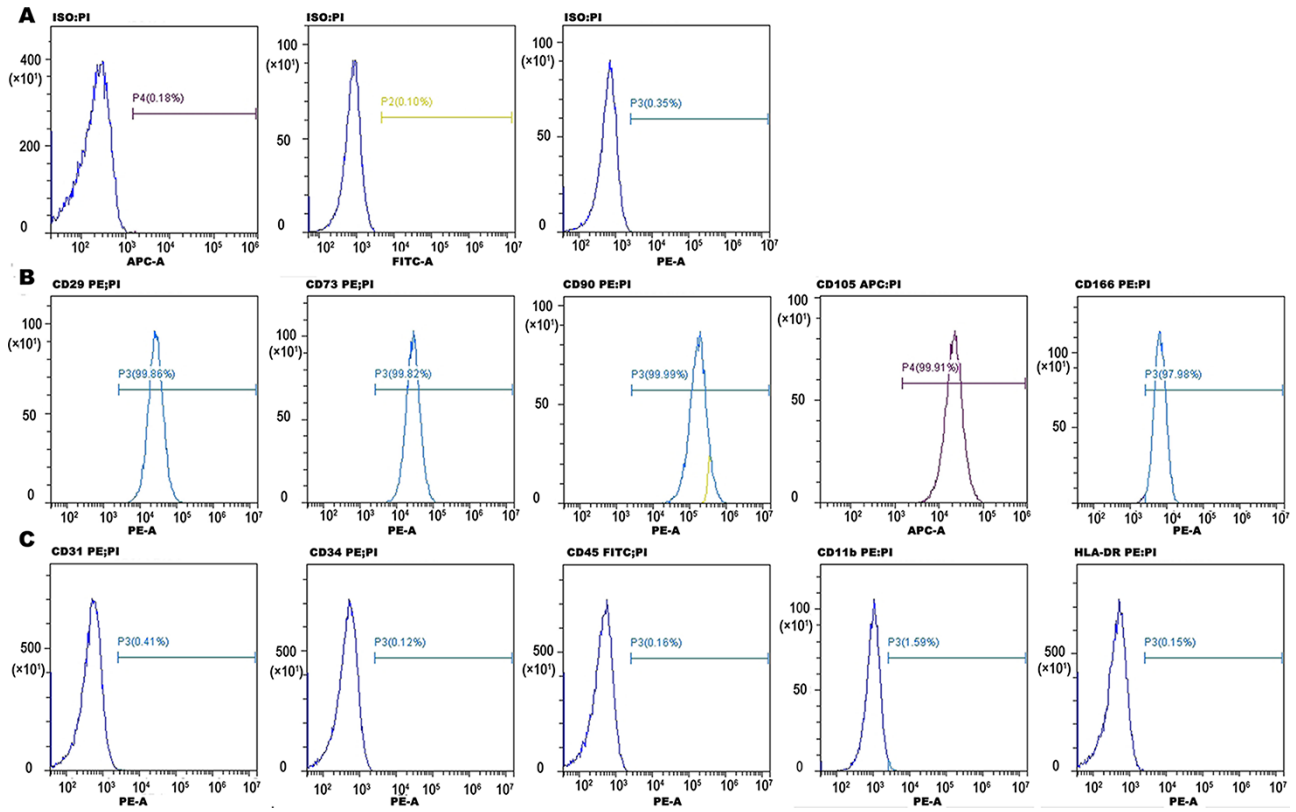

Figure 1. BMMSC surface markers were congruent with ISCT criteria BMMSC surface markers (CD29, CD73, CD90, CD105, CD166, CD31, CD34, CD45, CD11b, and HLA-DR) were analyzed by flow cytometry. (A) Isotype controls used in the experiment. (B) CD29, CD73, CD90, CD105, and CD166 were highly expressed in BMMSCs. (C) CD31, CD34, CD45, CD11b, and HLA-DR were almost not expressed in BMMSCs. The results demonstrated that the BMMSCs used in this study were in compliance with the criterion of the ISCT.

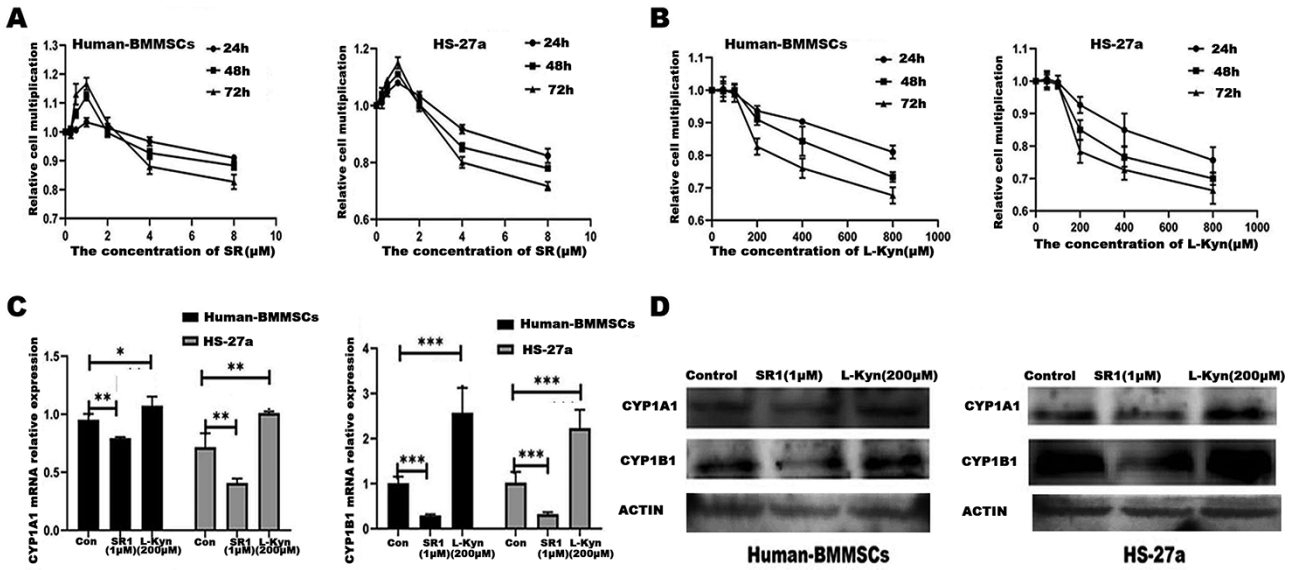

Figure 2. SR1 inhibited AHR activity and L-Kynurenine caused the activation of AHR in BMMSCs Relative cell proliferation was measured on a hemocytometer after incubation with different concentrations of SR1 or L-Kynurenine at 24, 48, and 72 h. (A) Cell proliferation was increased in time- and concentration-dependent manners after treatment with SR1 in BMMSCs and HS-27a cells. As the concentration of SR1 reached 1 μM, cell proliferation was greatly increased, and as the SR1 concentration was further increased, cell proliferation was reduced. (B) Cell proliferation was decreased in time- and concentration-dependent manners after treatment with L-Kynurenine. SR1 (1 μM) and L-Kynurenine (200 μM) were used in the subsequent experiments. The expression levels of CYP1A1 and CYP1B1 were detected by q-PCR and western blot analysis to determine the AHR activity at 48 h. (C) The mRNA expressions of *CYP1A1* and *CYP1B1* were decreased in the SR1 group compared with those in the L-Kynurenine and the control groups. After treatment with L-Kynurenine (200 μM), *CYP1A1* and *CYP1B1* mRNA expressions were higher than those in the control group. (D) The protein expressions of CYP1A1 and CYP1B1 were increased after treatment with L-Kynurenine (200 μM) and reduced after treatment with SR1 (1 μM). **P*<0.05, ***P*<0.01, ****P*<0.001 compared with the respective control group.

200 μM L-Kynurenine were used to inhibit and activate AHR in the experiment. The activation of AHR was monitored at 48 h by determining the expression levels of downstream promoters that contain AHR-binding sites such as CYP1A1 and CYP1B1. As shown in Fig. 2C,D, after AHR was inhibited by SR1 (1 μM), CYP1A1 and CYP1B1 mRNA and protein expression levels were significantly reduced. Meanwhile upon activation of AHR with L-Kynurenine (200 μM), their expressions were increased. These results suggested that L-Kynurenine (200 μM) activated AHR, while SR1 (1 μM) inhibited AHR.

AHR signaling was involved in the proliferation, apoptosis, and cell cycle of BMMSCs

We detected cell proliferation at 24 h and found that it was increased after BMMSCs or HS-27a cells were treated with SR1 (1 μM), while treatment with L-Kynurenine (200 μM) greatly decreased cell proliferation (Fig. 3A). There was no difference in cell apoptosis among the SR1, L-Kynurenine, and control groups (Fig. 3B). However, inhibition of AHR with SR1 (1 μM) promoted BMMSCs into the S phase of the cell cycle, and activation of the AHR with L-Kynurenine (200 μM) prevented the cells from passing the G1 phase (Fig. 3C). The mRNA expressions of cell-cycle-related proteins (cyclin-dependent kinases, CDKs) were detected by qPCR in BMMSCs at 48 h. CDK1, CDK2, CDK3, and CDK6 were expressed at higher levels in the SR1 group when compared with those in the control group or L-Kynurenine group (Fig. 3D). The expressions of CDK1, CDK2, CDK3, and CDK6 were decreased after treatment with L-Kynurenine (200 μM) in BMMSCs (Fig. 3D). Colony formation assay was used to explore the effect of AHR activation on BMMSCs. After the colonies were formed, they were stained with trypan blue and counted under the microscope. As shown in Fig. 3E, the inhibition of AHR led to an increase in the colony formation in both HS-27a cells and BMMSCs.

AHR expression was reduced in BMMSCs

To further explore the role of AHR signaling in BMMSCs, we knocked down AHR with AHR-siRNA. Forty-eight hours after transfection with the AHR-siRNA, AHR mRNA and protein levels were significantly downregulated (Fig. 4A,B). In the subsequent experiments, we used AHR-siRNA3 to knockdown AHR. As shown in Fig. 4C,D, AHR knockdown substantially decreased the expressions of CYP1A1 and CYP1B1 and reduced the effect of L-Kynurenine on the activation of AHR.

AHR knockdown facilitated BMMSC proliferation and promoted cell cycle progression to S phase

The reduction in AHR facilitated the proliferation of BMMSCs and promoted them to the S phase (Fig. 5A,C). Moreover, knockdown of AHR reduced the effect of L-Kynurenine on the proliferation and the cell cycle progression (Fig. 5A,C). As for apoptosis, no difference was observed after knocking down AHR in BMMSCs (Fig. 5B). The levels of CDKs were analyzed 48 h after knockdown of AHR, and the results showed that the expressions of CDK1, CDK2, CDK3, CDK4, and CDK6 were higher in BMMSCs, and AHR knockdown reduced the effect of L-Kynurenine on the expressions of CDKs (Fig. 5D).

AHR signaling regulated mitochondrial function

HS-27a cells and BMMSCs were incubated with SR1 (1 μM) and L-Kynurenine (200 μM) for 24, 48, and 72 h. The mitochondrial

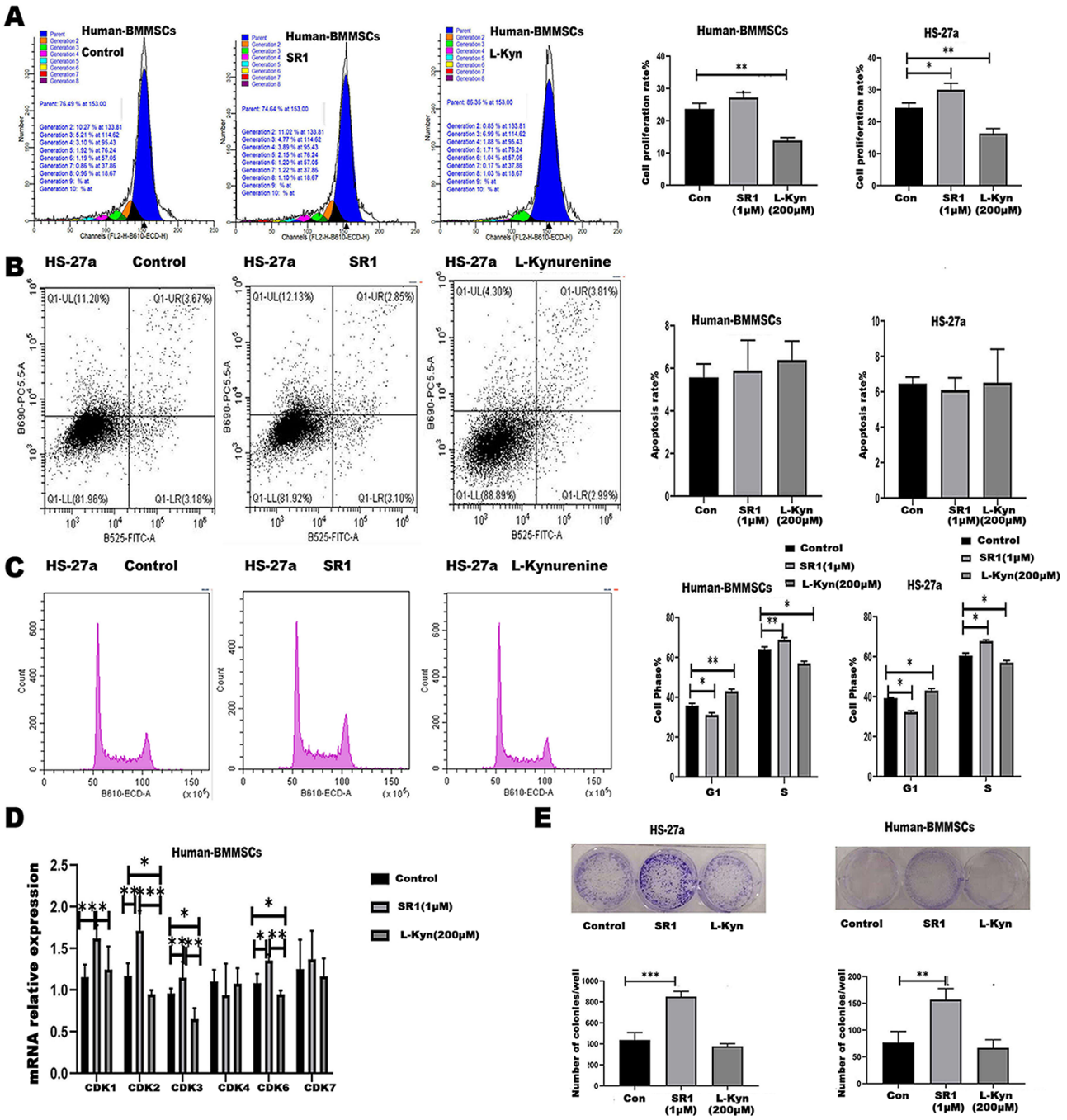

Figure 3. AHR activation was involved in the proliferation and cell cycle of BMMSCs Cell proliferation of BMMSCs was evaluated by flow cytometry. (A) Inhibiting AHR with SR1 (1 μM) at 24 h facilitated the proliferation of BMMSCs and HS-27a cells. Activating AHR with L-Kynurenine (200 μM) at 24 h decreased the proliferation. (B) There was no difference in BMMSCs apoptosis after treatment with SR1 (1 μM) or L-Kynurenine (200 μM) for 48 h. (C) Cell cycle kits were used to analyze the cell cycle of BMMSCs at 48 h: inhibiting AHR with SR1 (1 μM) promoted BMMSCs to the S phase and activating AHR with L-Kynurenine (200 μM) arrested cells in the G1 phase. (D) Expression levels of cell-cycle-related molecules were detected by q-PCR. The expression levels of *CDK1, CDK2, CDK3*, and *CDK6* were increased after inhibiting AHR with SR1 at 48 h, and their expression levels were decreased after treatment with L-Kynurenine (200 μM) for 48 h. (E) To further explore the effect of AHR activation on BMMSCs, BMMSC colonies were detected. BMMSCs and HS-27a cells were incubated with SR1 (1 μM) or L-Kynurenine (200 μM), and after 2 weeks, the colonies were detected. The results demonstrated that treatment with SR1 (1 μM) facilitated colony formation. **P*<0.05, ***P*<0.01, ****P*<0.001 compared with the respective control group.

dehydrogenase content was significantly decreased after treatment with SR1 (1 μM) and increased after treatment with L-Kynurenine (200 μM) in a time-dependent manner (Fig. 6A). Inhibiting AHR with SR1 (1 μM) increased the concentration of L-lactate, while activating AHR with L-Kynurenine (200 μM) decreased L-lactate concentration (Fig. 6B). We observed the color change of the medium containing phenol red and measured the pH value, which signified a change in cell metabolism. When cell oxidative phosphorylation

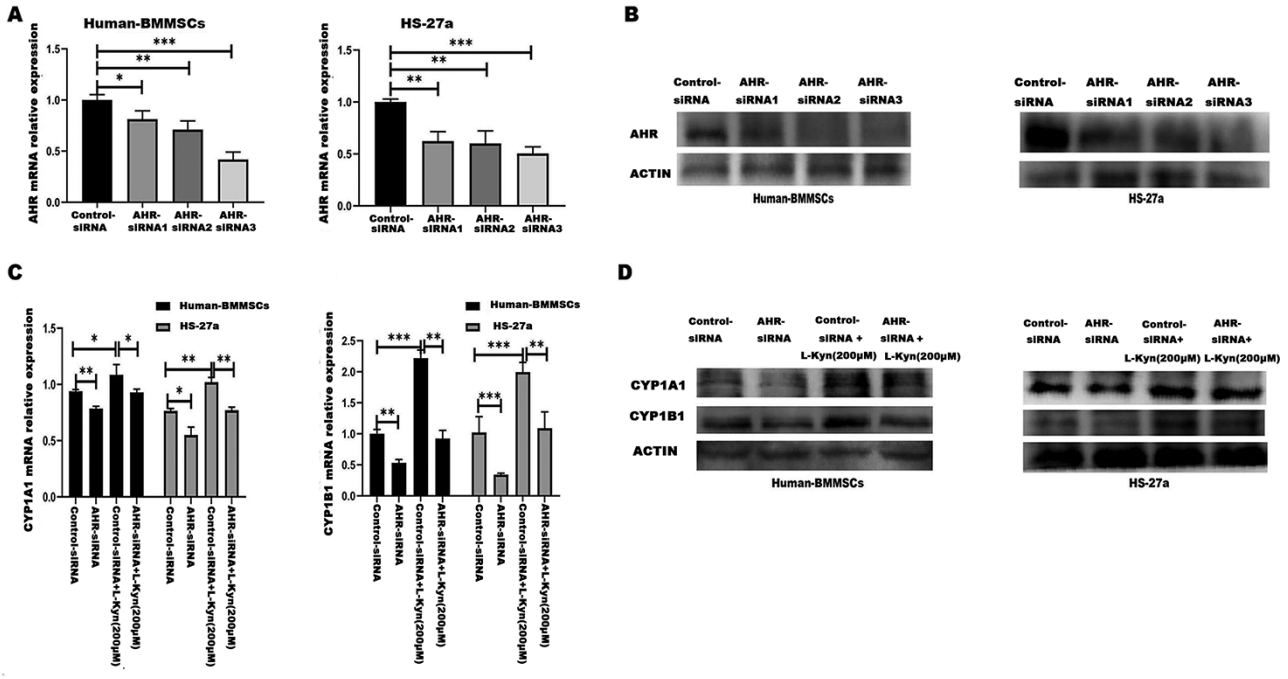

Figure 4. Reduce AHR expression with AHR-siRNA in BMMSCs AHR was knocked down with AHR-siRNA to further explore the roles of AHR in BMMSCs. (A,B) The mRNA and protein expression levels of AHR were reduced after AHR-siRNA transfection into BMMSCs and HS-27a cells at 48 h. (C,D) The downregulation of AHR decreased the expressions of CYP1A1 and CYP1B1. Treatment with L-Kynurenine (200 μM) did not increase the expressions of CYP1A1 and CYP1B1 after AHR was knocked down. **P*<0.05, ***P*<0.01, ****P*<0.001.

is weakened and glycolysis is enhanced, the acid content increases, the phenol red becomes lighter in color, and the pH value decreases. After incubation with SR1 (1 μM) and L-Kynurenine (200 μM) for 72 h, the medium containing phenol red in the SR1 group became lighter in color relative to the control and L-Kynurenine groups (Fig. 6C). We then measured the pH value and found that inhibiting AHR with SR1 significantly decreased the pH value compared with that of the control and L-Kynurenine groups, respectively (Fig. 6C).

After treatment with SR1 (1 μM) or L-Kynurenine (200 μM) for 48 h, the MMP of BMMSCs was detected. The results showed that the inhibition of AHR with SR1 decreased the MMP and the activation of AHR with L-Kynurenine increased the MMP (Fig. 6D). The levels of TFAM, which modulates mitochondrial oxidative phosphorylation and production, were detected in BMMSCs. After inhibiting AHR with SR1 for 48 h, the mRNA and protein expression levels of TFAM were decreased compared with that in the control group (Fig. 6E,F). Activation of the AHR with L-Kynurenine (200 μM) for 48 h increased the expression of TFAM compared with the control group (Fig. 6E,F).

AHR knockout in BMMSCs decreased mitochondrial function

To confirm the impact of AHR on mitochondrial function, we knocked down AHR with AHR-siRNA for 24, 48, and 72 h. We found that decreased AHR expression resulted in lower mitochondrial dehydrogenase levels and MMP but dramatically higher L-lactate levels in both BMMSCs and HS-27a cells (Fig. 7A–C). Interestingly, the decreased expression of the AHR attenuated the effect of L-Kynurenine on the mitochondrial function including mitochondrial dehydrogenase levels, MMP, and L-Lactate (Fig. 7A–C). After knocking down AHR for 48 h, the expression of mitochondrial-associated molecular TFAM was reduced (Fig. 7D,E). L-Kynurenine increased TFAM expression in BMMSCs, but after knockdown of the AHR, TFAM expression did not increase (Fig. 7D,E).

Discussion

BMMSCs have been explored as potential cell therapy agents in hematologic diseases because of their role in supporting hematopoiesis and modulating the immune system. These effects have been demonstrated *in vitro* and in several clinical trials [38,39]. BMMSCs are an important component of the bone marrow microenvironment, and their dysfunction is a pathogenesis-inducing factor in hematologic diseases [1]. Moreover, in hematologic diseases, BMMSCs show abnormalities, such as senescence, slow proliferation, and reduced differentiation potential [5,39]. The transfusion of normal BMMSCs into the bone marrow of patients with hematological diseases can reshape the bone marrow microenvironment and facilitate normal hematopoiesis [10,11]. Due to potential immune regulatory effects, BMMSCs have been used in the treatment and prevention of GVHD, which can improve the efficiency of bone marrow transplantation and survival rates [14–16].

For therapeutic applications, it is necessary to isolate and expand BMMSCs *in vitro*. Currently, the expansion of BMMSCs is performed under specific culture conditions and has certain limitations [40]. Recent studies have suggested that BMMSCs express AHR [20]. It has been reported that activation of AHR in NK cells results in impaired cell development and function [41]. Moreover, inhibition of the AHR promotes the expansion of hematopoietic progenitor cells and causes bone marrow failure [42]. In our previous study, we found that activation of AHR altered the metabolism of acute myeloid leukemia (AML) cells and kept them

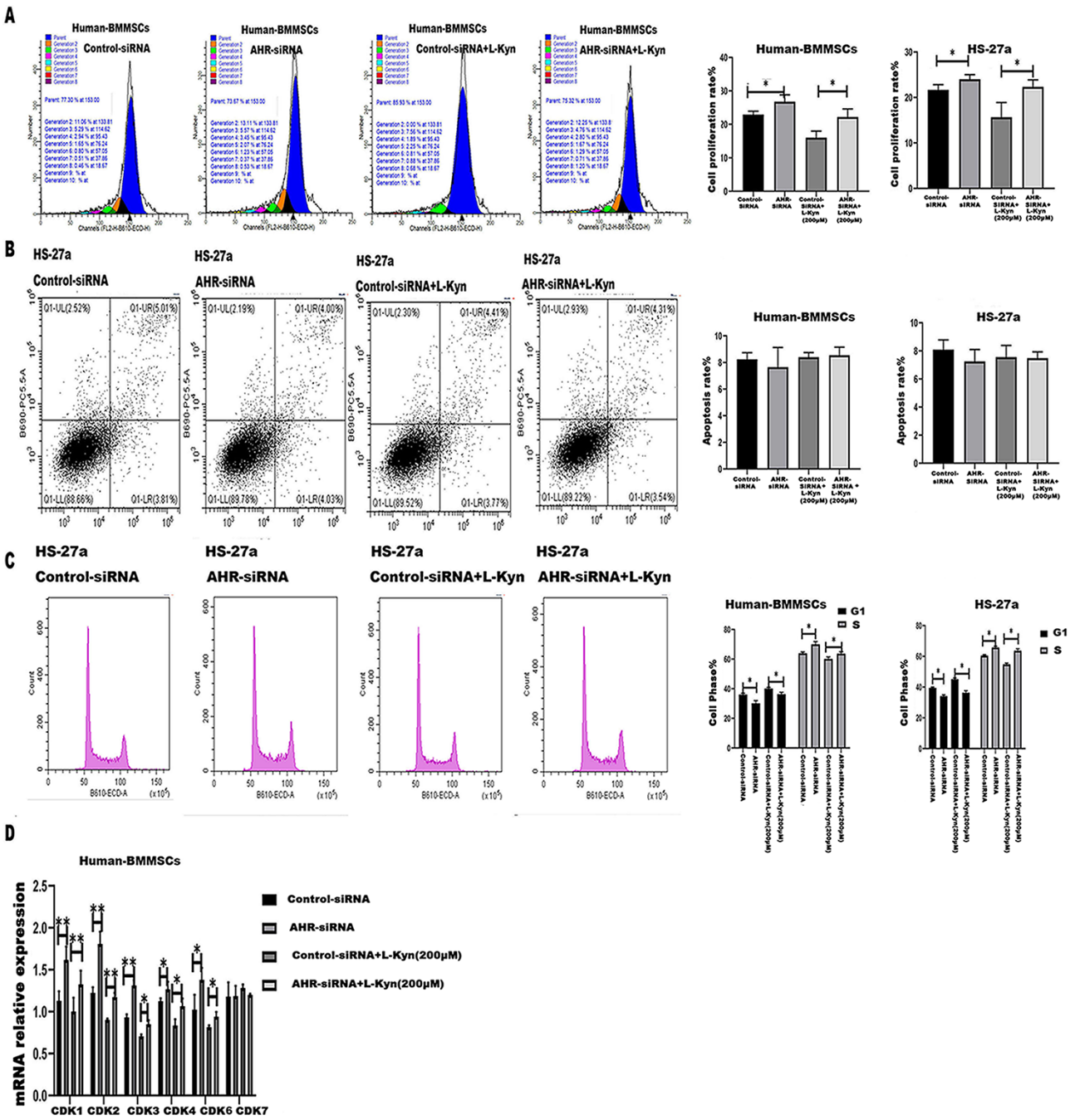

Figure 5. Reduced AHR expression promoted the proliferation and cell cycle of BMMSCs The AHR was knocked down with AHR-siRNA. (A–C) Knocking down AHR with AHR-siRNA led to the increase in cell proliferation and the promotion of the BMMSC and HS-27a cell cycle to the S phase, but no difference in apoptosis was seen among these groups. After knockdown of AHR, treatment with L-Kynurenine (200 μM) in BMMSCs and HS-27a cells did not restore the proliferation or cell cycle. (D) The reduction in AHR caused increased expressions of cell-cycle-associated molecules (CDK1, CDK2, CDK3, CDK4, and CDK6) and reduced the effects of L-Kynurenine on BMMSCs and HS-27a cells. **P*<0.05, ***P*<0.01 compared with the respective control group.

quiescent, which induced cytarabine resistance [33]. However, the role of AHR in BMMSCs remains unclear. CYP1A1 and CYP1B1 are classical downstream molecules of the AHR signaling pathway, and their increased expressions indicate the activation of AHR [43]. In the present study, treatment of BMMSCs and HS-27 cells with L-Kynurenine led to higher CYP1A1 and CYP1B1 expressions compared to those in the SR1 group or control group. After BMMSCs and HS-27 cells were treated with SR1, the expressions of CYP1A1 and CYP1B1 were decreased. The results showed that L-Kynurenine activated AHR, whereas SR1 inhibited AHR. Activation of AHR in BMMSCs and HS-27a cells with L-Kynurenine inhibited cell proliferation and arrested BMMSCs and HS-27a cells in the G1 phase, while inhibiting AHR with SR1 had the opposite result. Moreover, when AHR was knocked down with AHR-siRNA, cell proliferation was increased and BMMSCs and HS-27a cells were promoted into the S phase. Interestingly, the reduction in AHR attenuated the

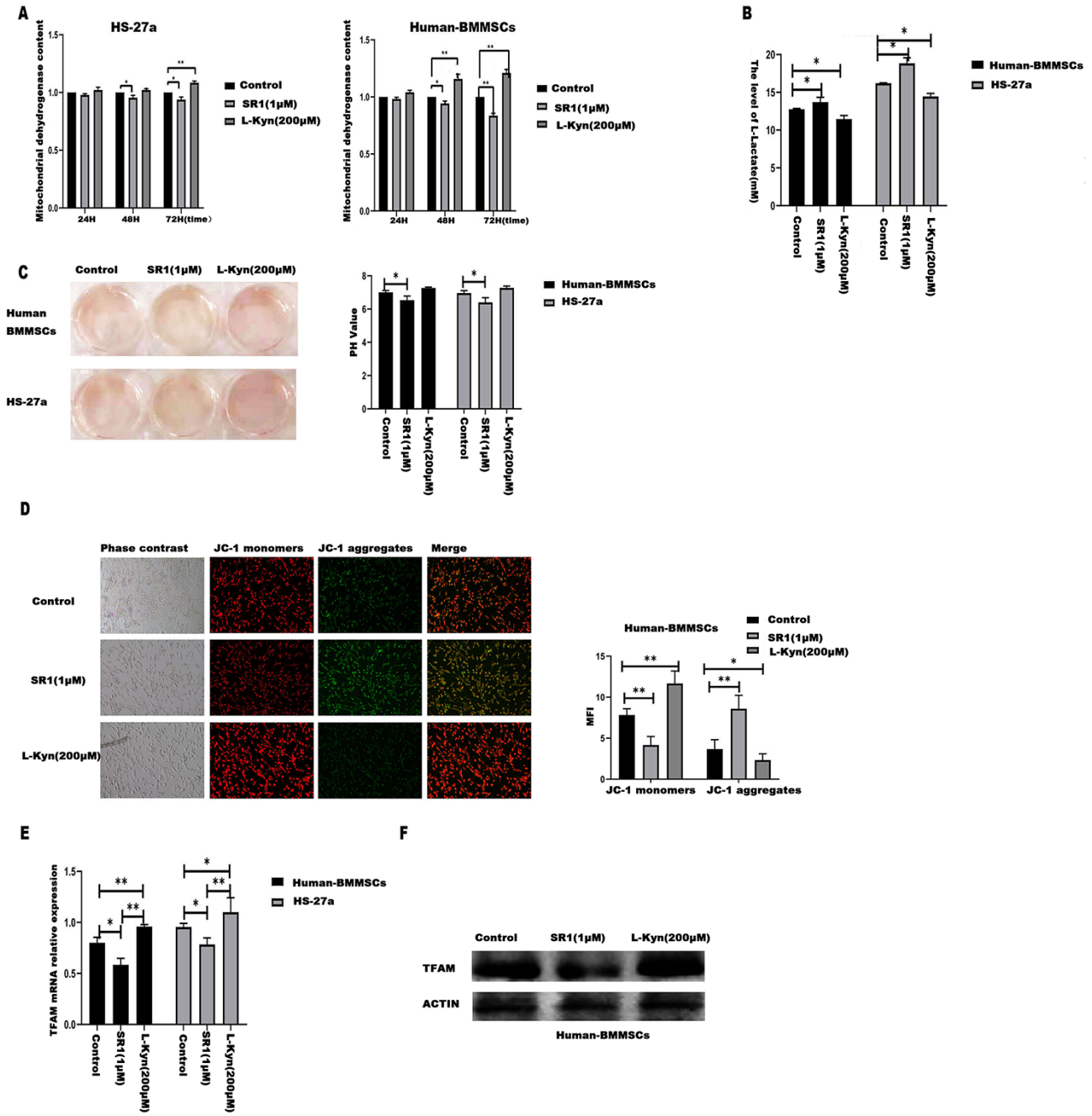

Figure 6. Activation of AHR altered mitochondrial function (A,B,D) Activating AHR with L-Kynurenine (200 μM) enhanced mitochondrial function, as demonstrated by increased levels of mitochondrial dehydrogenase and MMP and decreased L-lactate level. Inhibiting AHR with SR1 (1 μM) produced the opposite effect. Magnifiction, 10x. (C) Incubating BMMSCs and HS-27a cells with SR1 (1 μM) for 72 h reduced the pH of cell metabolites, and treatment with L-Kynurenine (200 μM) for 72 h increased the pH of cell metabolites. (E,F) After inhibiting the AHR with SR1 for 48 h, the mRNA and protein expression levels of TFAM were decreased compared with those in the control groups. Activation of the AHR with L-Kynurenine (200 μM) for 48 h increased the expression of TFAM compared with that in the control group. *P<0.05, **P<0.01 compared with the respective control group.

effect of L-Kynurenine. These results revealed that the AHR signal pathway is involved in BMMSC proliferation and cell cycle.

AHR attenuates oxidative-stress-induced cell injury by maintaining the structural and functional stability of mitochondria [21,22,44]. Zhou *et al*. [24] found that knocking down the AHR gene in mast cells resulted in damage to mitochondrial function, including uncoupling of the mitochondrial electron transport chain. TFAM is an essential mtDNA packaging protein that is required for mtDNA transcription and replication and is involved in oxidative phosphorylation [26,27,32]. In AML and melanocyte cells, activation of AHR enhanced mitochondrial function through TFAM [33]. There have been few reports on the regulation of mitochondria by AHR in BMMSCs. However, we found that activation of AHR with L-Kynurenine enhanced mitochondrial function, as shown by the increased levels of mitochondrial dehydrogenase content and MMP and decreased lactate level. Inhibition of AHR with

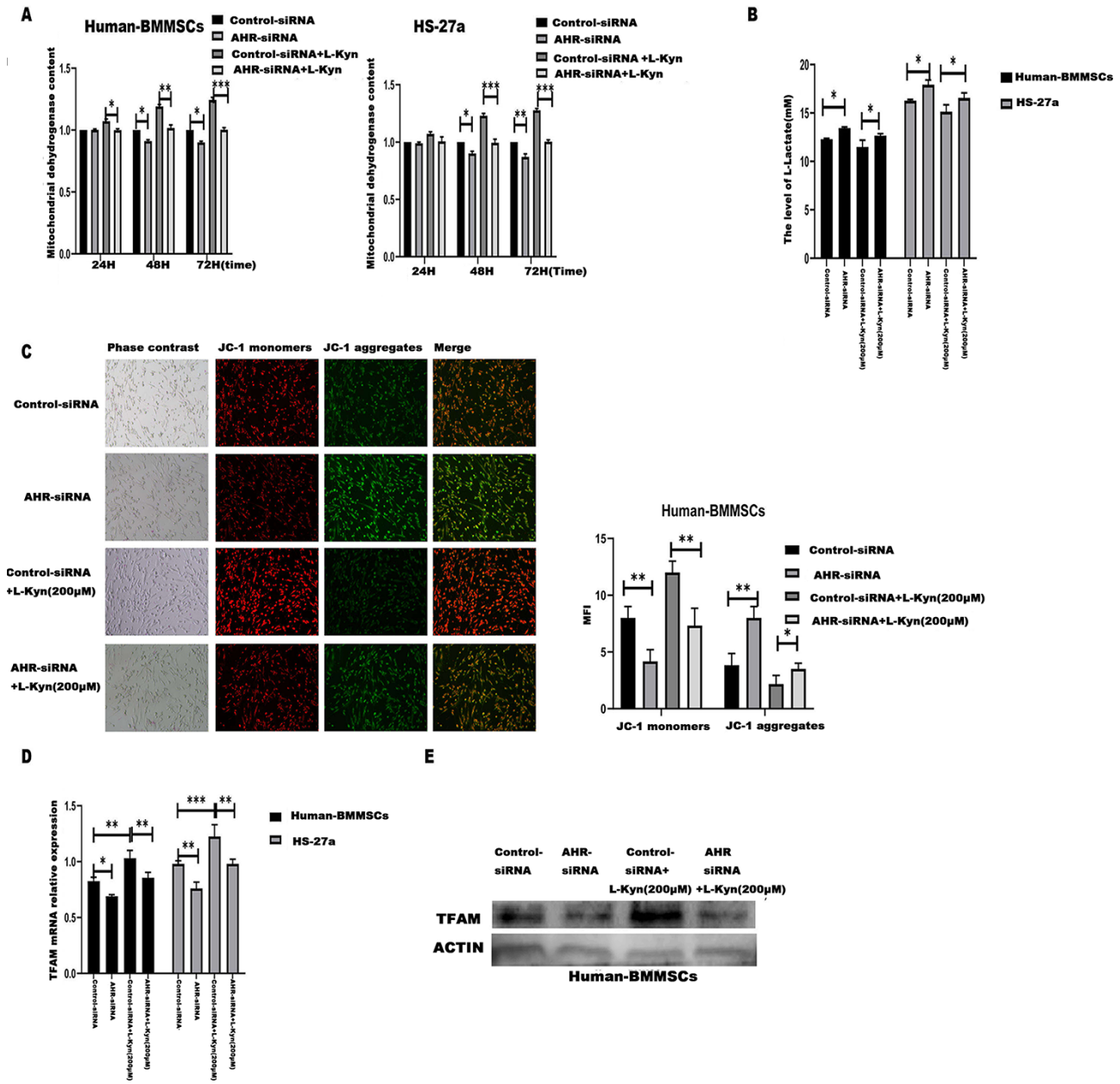

Figure 7. Reduction in AHR alleviated mitochondrial function (A–C) Knockdown of AHR decreased mitochondrial function, including decreased levels of mitochondrial dehydrogenase and MMP, and increased L-lactate level. The reduction in AHR decreased the effect of L-Kynurenine. Magnification, 10x. (D,E) Reduced AHR expression decreased mitochondrial-associated TFAM level and decreased the effect of L-Kynurenine (200 μM) on BMMSCs and HS-27a cells. **P*<0.05, ***P*<0.01, ****P*<0.001 compared with the respective control group.

SR1 decreased mitochondrial function. Furthermore, after activation of AHR, the expression of TFAM was increased, while inhibition of AHR decreased TFAM expression. Furthermore, knockdown of AHR with AHR-siRNA led to decreased mitochondrial function. Therefore, our results demonstrated that AHR signaling is associated with mitochondrial function in BMMSCs.

Accumulating evidence demonstrated that the upregulation of mitochondrial function and the metabolic shift are essential for the differentiation and therapeutic effects of BMMSCs [28,36,37]. Mitochondrial metabolism is well known to be involved in the proliferative behaviors of cells. Glycolysis provides sufficient materials and energy for cell proliferation; however, enhanced oxidative phosphorylation in cells increases catabolism and reduces anabolism, which cannot meet the needs of cell proliferation, resulting in the cell cycle being blocked or the cell becoming quiescent. Activation of AHR in HSCs was found to promote the cells into the quiescent state [33]. Furthermore, Liu *et al*. [45] demonstrated that cancer cells enter a dormant state via interferon-γ-IDO1-AhR signaling pathway to avoid the killing effects of chemotherapy drugs. However, the exact mechanism is still unclear. In the present study, we found that activation of AHR inhibited the proliferation of BMMSCs and enhanced their mitochondrial function. We can conclude that activation of AHR in BMMSCs altered the mitochondrial function and thereby influenced the proliferative behaviors of cells.

In conclusion, AHR activation is involved in the proliferation and metabolism of BMMSCs. This study may provide the basis for further unveiling the molecular mechanisms and therapeutic potential of AHR in BMMSCs.

Funding

This work was support by the grants from the National Science Foundation of China (Nos. 81570108 and 81400090).

Conflict of Interest

The authors declare that they have no conflict of interest.

References

1. Zheng Q, Zhao Y, Guo J, Zhao S, Fei C, Xiao C, Wu D, *et al.* Iron overload promotes mitochondrial fragmentation in mesenchymal stromal cells from myelodysplastic syndrome patients through activation of the AMPK/MFF/Drp1 pathway. *Cell Death Dis* 2018, 9: 515.
2. Okabe H, Suzuki T, Uehara E, Ueda M, Nagai T, Ozawa K. The bone marrow hematopoietic microenvironment is impaired in iron-overloaded mice. *Eur J Haematol* 2014, 93: 118–128.
3. Naji A, Eitoku M, Favier B, Deschaseaux F, Rouas-Freiss N, Suganuma N. Biological functions of mesenchymal stem cells and clinical implications. *Cell Mol Life Sci* 2019, 76: 3323–3348.
4. Starc N, Ingo D, Conforti A, Rossella V, Tomao L, Pitisci A, De Mattia F, *et al.* Biological and functional characterization of bone marrow-derived mesenchymal stromal cells from patients affected by primary immunodeficiency. *Sci Rep* 2017, 7: 8153.
5. Shi L, Zhao Y, Fei C, Guo J, Jia Y, Wu D, Wu L, *et al.* Cellular senescence induced by S100A9 in mesenchymal stromal cells through NLRP3 inflammasome activation. *Aging (Albany NY)* 2019, 11: 9626–9642.
6. Zhao Y, Wu D, Fei C, Guo J, Gu S, Zhu Y, Xu F, *et al.* Down-regulation of Dicer1 promotes cellular senescence and decreases the differentiation and stem cell-supporting capacities of mesenchymal stromal cells in patients with myelodysplastic syndrome. *Haematologica* 2015, 100: 194–204.
7. Guo J, Zhao Y, Fei C, Zhao S, Zheng Q, Su J, Wu D, *et al.* Dicer1 downregulation by multiple myeloma cells promotes the senescence and tumor-supporting capacity and decreases the differentiation potential of mesenchymal stem cells. *Cell Death Dis* 2018, 9: 512.
8. Crippa S, Rossella V, Aprile A, Silvestri L, Rivis S, Scaramuzza S, Pirroni S, *et al.* Bone marrow stromal cells from β-thalassemia patients have impaired hematopoietic supportive capacity. *J Clin Invest* 2019, 129: 1566–1580.
9. Burt R, Dey A, Aref S, Aguiar M, Akarca A, Bailey K, Day W, *et al.* Activated stromal cells transfer mitochondria to rescue acute lymphoblastic leukemia cells from oxidative stress. *Blood* 2019, 134: 1415–1429.
10. Xia C, Wang T, Cheng H, Dong Y, Weng Q, Sun Q, Zhou P, *et al.* Mesenchymal stem cells suppress leukemia via macrophage-mediated functional restoration of bone marrow microenvironment. *Leukemia* 2020, 34: 2375–2383.
11. Fattizzo B, Giannotta JA, Barcellini W. Mesenchymal stem cells in aplastic anemia and myelodysplastic syndromes: the 'seed and soil' crosstalk. *Int J Mol Sci* 2020, 21: 5438.
12. Zhao L, Chen S, Yang P, Cao H, Li L. The role of mesenchymal stem cells in hematopoietic stem cell transplantation: prevention and treatment of graft-versus-host disease. *Stem Cell Res Ther* 2019, 10: 182.
13. Jamil MO, Mineishi S. State-of-the-art acute and chronic GVHD treatment. *Int J Hematol* 2015, 101: 452–466.
14. Fierabracci A, Del FA, Muraca M, Delfino DV, Muraca M. The use of mesenchymal stem cells for the treatment of autoimmunity: from animals models to human disease. *Curr Drug Targets* 2016, 17: 229–238.
15. Uccelli A, Moretta L, Pistoia V. Immunoregulatory function of mesenchymal stem cells. *Eur J Immunol* 2006, 36: 2566–2573.
16. Devine SM, Hoffman R. Role of mesenchymal stem cells in hematopoietic stem cell transplantation. *Curr Opin Hematol* 2000, 7: 358–363.
17. Dazzi F, Ramasamy R, Glennie S, Jones SP, Roberts I. The role of mesenchymal stem cells in haemopoiesis. *Blood Rev* 2006, 20: 161–171.
18. Wang S, Qu X, Zhao RC. Clinical applications of mesenchymal stem cells. *J Hematol Oncol* 2012, 5: 19.
19. Jia Y, Zhang C, Hua M, Wang M, Chen P, Ma D. Aberrant NLRP3 inflammasome associated with aryl hydrocarbon receptor potentially contributes to the imbalance of T-helper cells in patients with acute myeloid leukemia. *Oncol Lett* 2017, 14: 7031–7044.
20. Abney KK, Galipeau. J. Aryl hydrocarbon receptor in mesenchymal stromal cells: new frontiers in AhR biology. *FEBS J* 2021, 288: 3962–3972.
21. Zhou B, Wang X, Li F, Wang Y, Yang L, Zhen X, Tan W. Mitochondrial activity and oxidative stress functions are influenced by the activation of AhR-induced CYP1A1 overexpression in cardiomyocytes. *Mol Med Rep* 2017, 16: 174–180.
22. Rico DA, Zago M, Pollock SJ, Sime PJ, Phipps RP, Baglole CJ. Genetic ablation of the aryl hydrocarbon receptor causes cigarette smoke-induced mitochondrial dysfunction and apoptosis. *J Biol Chem* 2011, 286: 43214–43228.
23. Wu R, Zhang L, Hoagland MS, Swanson HI. Lack of the aryl hydrocarbon receptor leads to impaired activation of AKT/protein kinase B and enhanced sensitivity to apoptosis induced via the intrinsic pathway. *J Pharmacol Exp Ther* 2007, 320: 448–457.
24. Zhou Y, Tung H, Tsai Y, Hsu S, Chang H, Kawasaki H, Tseng H, *et al.* Aryl hydrocarbon receptor controls murine mast cell homeostasis. *Blood* 2013, 121: 3195–3204.
25. Zhang Y, Marsboom G, Toth PT, Rehman J. Mitochondrial respiration regulates adipogenic differentiation of human mesenchymal stem cells. *PLoS One* 2013, 8: e77077.
26. Kang I, Chu CT, Kaufman BA. The mitochondrial transcription factor TFAM in neurodegeneration: emerging evidence and mechanisms. *FEBS Lett* 2018, 592: 793–811.
27. Campbell CT, Kolesar JE, Kaufman BA. Mitochondrial transcription factor a regulates mitochondrial transcription initiation, DNA packaging, and genome copy number. *Biochim Biophys Acta* 2012, 1819: 921–929.
28. Lee JY, Lee DC, Im JA, Lee JW. Mitochondrial DNA copy number in peripheral blood is independently associated with visceral fat accumulation in healthy young adults. *Int J Endocrinol* 2014, 2014: 586017.
29. Filograna R, Mennuni M, Alsina D, Larsson N. Mitochondrial DNA copy number in human disease: the more the better? *FEBS Lett* 2021, 595: 976–1002.
30. Bauerfeld C, Talwar H, Zhang K, Liu Y, Samavati L. MKP-1 modulates mitochondrial transcription factors, oxidative phosphorylation, and glycolysis. *Immunohorizons* 2020, 4: 245–258.
31. Elswood J, Pearson S, Payne R, Barhoumi R, Rijnkels M, Porter W. Autophagy regulates functional differentiation of mammary epithelial cells. *Autophagy* 2021, 17: 420–438.
32. Wang X, Li S, Liu L, Jian Z, Cui T, Yang Y, Guo S, *et al.* Role of the aryl hydrocarbon receptor signaling pathway in promoting mitochondrial biogenesis against oxidative damage in human melanocytes. *J Dermatol Sci* 2019, 96: 33–41.
33. Jia Y, Guo J, Zhao Y, Zhang Z, Shi L, Fang Y, Wu D. AHR signaling pathway reshapes the metabolism of AML/MDS cells and potentially leads to cytarabine resistance. *Acta Biochim Biophys Sin* 2021, 53: 492–500.
34. Thaweesapphithak S, Tantrawatpan C, Kheolamai P, Tantikanlayaporn D, Roytrakul S, Manochantr S, Thaweesapphithak S, *et al.* Human serum enhances the proliferative capacity and immunomodulatory property of MSCs derived from human placenta and umbilical cord. *Stem Cell Res Ther* 2019, 10: 79.
35. Hsu Y, Wu Y, Yu T, Wei Y. Mitochondria in mesenchymal stem cell biology and cell therapy: from cellular differentiation to mitochondrial transfer. *Semin Cell Dev Biol* 2016, 52: 119–131.
36. Wanet A, Arnould T, Najimi M, Renard P. Connecting mitochondria, metabolism, and stem cell fate. *Stem Cells Dev* 2015, 24: 1957–1971.
37. Taketani T. Clinical application of mesenchymal stem cells for hematological diseases. *Rinsho Ketsueki* 2018, 59: 2362–2372.

38. Zhao L, Chen S, Yang P, Cao H, Li L. The role of mesenchymal stem cells in hematopoietic stem cell transplantation: prevention and treatment of graft-versus-host disease. *Stem Cell Res Ther* 2019, 10: 182.
39. Fei C, Guo J, Zhao Y, Zhao S, Zhen Q, Shi L, Li X, *et al*. Clinical significance of hyaluronan levels and its pro-osteogenic effect on mesenchymal stromal cells in myelodysplastic syndromes. *J Transl Med* 2018, 16: 234.
40. Aboulghassem S, Katrine F, Terje H, Finn PR, Jan EB. *In vitro* expansion of human mesenchymal stem cells: choice of serum is a determinant of cell proliferation, differentiation, gene expression, and transcriptome stability. *Stem Cell* 2005, 23: 1357–1366.
41. Scoville S, Nalin A, Chen L, Chen L, Zhang M, McConnell K, Casas S, *et al*. Human AML activates the aryl hydrocarbon receptor pathway to impair NK cell development and function. *Blood* 2018, 132: 1792–1804.
42. Lindsey S, Papoutsakis E. The evolving role of the aryl hydrocarbon receptor (AHR) in the normophysiology of hematopoiesis. *Stem Cell Rev Rep* 2012, 8: 1223–1235.
43. Schiering C, Wincent E, Metidji A, Iseppon A, Li Y, Potocnik A, Omenetti S, *et al*. Feedback control of AHR signalling regulates intestinal immunity. *Nature* 2017, 542: 242–245.
44. Wang X, Li S, Ling L, Jian Z, Cui T, Yang Y, Guo S, *et al*. Role of the aryl hydrocarbon receptor signaling pathway in promoting mitochondrial biogenesis against oxidative damage in human melanocytes. *J Dermatol Sci* 2019, 96: 33–41.
45. Liu Y, Liang X, Yin X, Lv J, Tang K, Ma J, Ji T, *et al*. Blockade of IDO-kynurenine-AhR metabolic circuitry abrogates IFN-γ-induced immunologic dormancy of tumor-repopulating cells. *Nat Commun* 2017, 8: 15207.